SLAC–PUB–6232
September 1993
(A)

Simulation and Analysis of RF Feedback Systems on the SLC Damping Rings

M. Minty, T. Himel, P. Krejcik, R.H. Siemann, R. Tighe

Stanford Linear Accelerator Center, Stanford University, Stanford, CA 94309, USA

Abstract

The rf system of the SLC Damping Rings has evolved since tighter tolerances on beam stability are encountered as beam intensities are increased. There are now many feedback systems controlling the phase and amplitude of the rf, the phase of the beam, and the tune of the cavity. The bandwidths of the feedback loops range from several MHz to compensate for beam loading to a few Hz for the cavity tuners. To improve our understanding of the interaction of these loops and verify their expected behavior, we have simulated their behavior using computer models. A description of the models and the first results are discussed.

1. Introduction

During the 1992 SLC/SLD run, accelerator operation became sensitive to the microwave instability[1] at beam currents above 3×10^{10} particles per bunch. To avoid the onset of bunch lengthening at higher currents, an rf voltage ramp was implemented. However, the depth of the ramp was limited by a Robinson-like instability[2,3], which was corrected for using direct rf feedback[3,4]. With these modifications, the parameter space has become more complex. Operating conditions must be adjusted and optimized such that the rf system operates stably under varying conditions. In particular, the system should be insensitive to injection phase errors and intensity jitter, repetition rate changes, and effects arising from klystron saturation.

Effects of heavy beam loading and rf feedback have been studied in detail by Pedersen[2,3], who has also studied the effect of adding more feedback loops. The dynamics become more complicated when the nonlinear effects of klystron saturation are considered. The purpose of our simulations is to understand the stability of the damping ring rf system with multiple feedback loops and a partially saturated klystron.

2. System Overview

A block diagram of the rf system is shown in Fig. 1. The coupling between the beam and cavities increases as the beam current is raised. Two cavities are driven by a single klystron. Surrounding the cavities and klystron are various feedback loops. The cavity voltage is regulated using the gap voltage control feedback. Other loops include a beam loading feedback, a beam phase loop, a klystron phase compensation loop, a synchrotron oscillation zero mode feedback, and cavity tuner loops.

*Work supported by the Department of Energy Contract DE-AC03-76SF00515

The rf system is modelled by calculating the dynamics of the beam cavity interaction. These equations along with measured loop characteristics and klystron saturation data are then incorporated into numerical integration programs such as Matrix-x[5] and Simulink[6]. These algorithms use state space representations of the system to solve the differential equations. The system can be analyzed in both the time and frequency domains.

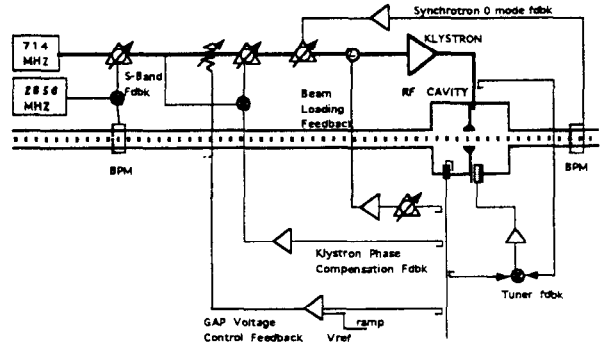

Figure 1. SLC damping ring rf system.

3. System Modelling

We first discuss the beam cavity interaction and the klystron. We then consider the various feedback loops.

A. Beam Cavity Interaction

The equations of motion for the beam cavity interaction are mixed to baseband for computational efficiency. Each cavity is modelled as a parallel RLC circuit. The dynamics are described by

$$\frac{dv_r}{dt}+\frac{1}{2Q}\frac{dv_i}{dt}+\frac{v_r}{2Q}\omega_{rf}+v_i(\omega_0-\omega_{rf})=\frac{R\omega_{rf}}{2Q}I_r$$

$$\frac{dv_i}{dt}-\frac{1}{2Q}\frac{dv_r}{dt}+\frac{v_i}{2Q}\omega_{rf}-v_r(\omega_0-\omega_{rf})=\frac{R\omega_{rf}}{2Q}I_i \quad (1)$$

Here v_r and v_i are the real and imaginary parts of the cavity voltage and the approximation $\frac{dv}{dt}\ll v\omega_{rf}$ has been made. Also $Q=6860$ is the loaded quality factor of the cavities, $\omega_{rf}=2\pi\times 714$ MHz is the angular drive frequency, $R=2.5$ MΩ is the shunt impedance, I_r and I_i are the real and imaginary parts of the total current, $I_t=I_g+I_b$, where I_g is the generator and I_b is the beam current. The resonant frequency, ω_0, of the cavity is given by $\frac{\omega_0}{\omega_{rf}}=[1-\frac{1}{2Q}\tan\phi_z]^{-1}$, where ϕ_z is the impedance angle between the total current and the cavity voltage.

Presented at the Particle Accelerator Conference (PAC93), Washington DC, May 17–20, 1993

The equations for the beam current, expressed in polar coordinates, are $|I_b| = 2I_{dc}$, where I_{dc} is the dc beam current and, for the nonlinear phase equation,

$$\frac{d^2\phi_b}{dt^2} = -\frac{\eta\omega_{rf}}{E_0 T_0}[|V|\sin\phi_b - (U_0 + U_{hom})], \qquad (2)$$

in which ϕ_b is the beam phase angle, ϕ_c is the cavity phase angle, $\eta = -0.015$ is the slip factor, $E_0 = 1.19$ GeV is the beam energy, $T_0 = \frac{2\pi}{\omega rf} = 117.65$ ns is the revolution period, and U_0 and U_{hom} are respectively the energy losses due to synchrotron radiation and higher order modes.

An example of the time dependence of the beam phase is shown in the insert of Fig. 2. With the impedance angle ϕ_z equal to -20 degrees, the damping time τ of the oscillations is compared with analytic calculation.

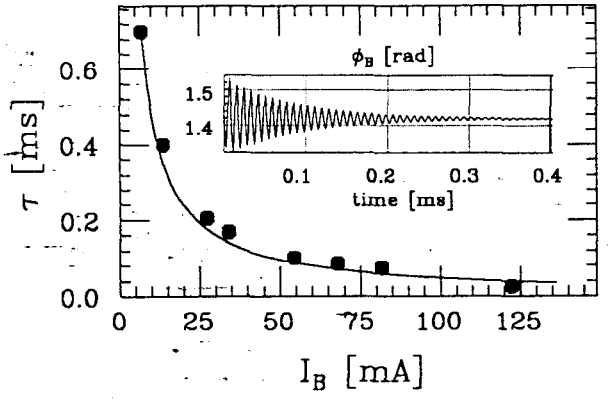

Figure 2. Damping time of phase oscillations as a function of beam current with $\phi_z = -20$ deg. A simulation output of the beam phase for I_B=68 mA is also shown.

B. Nonlinear Klystron

To minimize the bunch length at extraction we operate the klystrons in the nonlinear region near saturation. The measured saturation characteristics of the klystron are shown in Fig. 3. The klystron becomes nonlinear in gain at an output power near 30 kW or at a cavity voltage of 550 kV when tuned for optimum coupling. In addition, the klystron produces a power dependent phase offset for output powers greater than 10 kW. These data are input into the model in the form of interpolation tables. The klystron bandwidth (5.3 Mhz at 3 dB) is modelled at baseband as a third order lowpass Butterworth filter. A 240 ns delay is also included. To compute the output current I_g we convert the input voltage V_{in} into input power P_{in}, use the saturation data to determine the output power P_{out}, and take into account the coupling to the cavity ($\beta = 2.5$). The transconductance, S, for which $I_g = SV_{in}$, is

$$S = \sqrt{\frac{4\beta}{(1+\beta)^2}\frac{1}{2R(50\Omega)}\left(\frac{P_{out}}{P_{in}}\right)} \qquad (3)$$

The phase shift resulting from driving the klystron to saturation is also calculated from the input power.

The open loop Bode plot obtained by modulating the klystron input and detecting the amplitude controller output (see below) is shown in Fig. 4 and is compared with online measurement. From the figure can be seen the additive effects of the cavities and the klystron as well as the controller and rf attenuator on the system gain and phase.

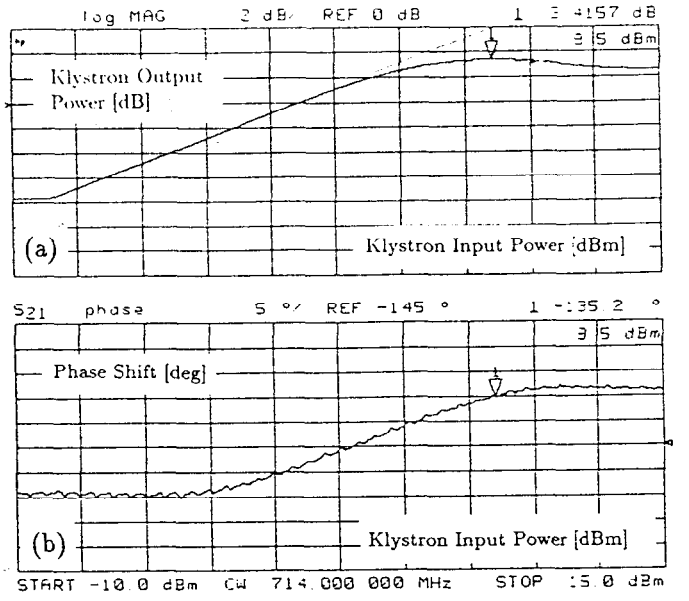

Figure 3. Measured gain (fig. 3a) and phase shift (fig. 3b) of klystron as a function of input power.

C. Feedback Loops

Beam Loading Feedback

The rf feedback loop is described in detail in Ref. 4. When this feedback is implemented, the Q of the cavity is reduced by $1+G_0$, where G_0 is the feedback gain. In the model, we form the vector sum of the two cavity voltages and allow an overall phase shift of the feedback signal. A 120 ns delay is included for the waveguides and cable delays. Simulations to determine the threshold for unstable exponential growth of phase oscillations agree well with theory.

Amplitude Feedback Loop

The amplitude feedback loop is used to regulate the voltage ramp during the store cycle. Unlike the rf feedback, which uses the vector sum of the cavity voltages as the feedback signal, the amplitude loop feeds back on the sum of the magnitude of the two cavity voltages. The measured 3 dB bandwidth of the controller is about 600 Hz. A first order transfer function characterizes its frequency response. In addition, we model a series rf attenuator as a first order transfer function with the measured 3 dB bandwidth of 40 kHz. When the rf feedback loop is closed, the gain in the amplitude feedback is raised by $1 + G_0$ accordingly.

Phase Feedback Loop

The phase loop is used to lock the ring rf at extraction to the linear accelerator rf. We model it as a constant gain bandwidth amplifier and use a first order transfer function with a measured 3 dB bandwidth of 30 Hz.

Klystron Compensation Feedback Loop

This phase feedback loop is supposed to compensate for

slow variations in the AC power source for the klystron drive. The measured 3 dB bandwidth is about 10 Hz.

Cavity Tuner Loop

The very slow ($\leq$1 Hz) tuner loop is used primarily to control the initial conditions for the loading angle ϕ_l. The phase angle ϕ_z between the cavity and generator is fed back through a second order transfer function.

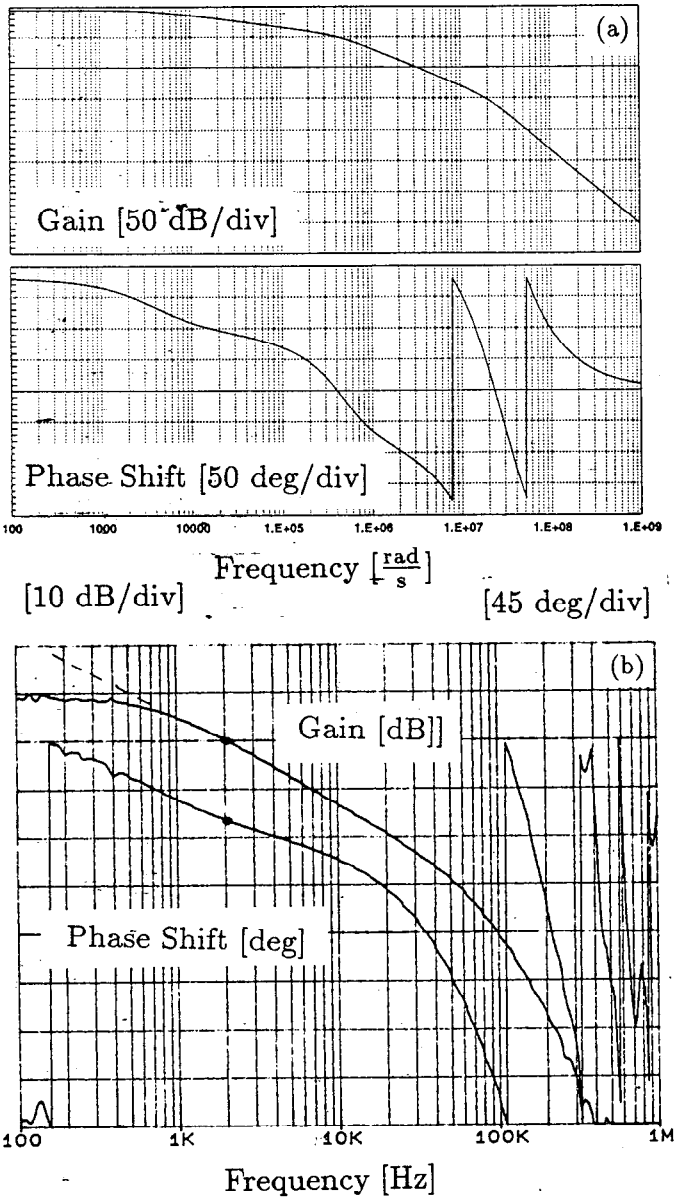

Figure 4. Calculated open loop response (fig. 4a) is compared with online measurement (fig. 4b)

4. Effect of Nonlinear Klystron

The saturation in the klystron reduces the stability threshold for the system as there is insufficient output power to compensate for heavy beam loading. Plotted in Fig. 5a is the ratio of the klystron output to input power as a function of the beam loading ratio, $Y = \frac{I_B R}{V}$, for different cavity voltages with all feedback loops off. The impedance angle was held fixed at -45 degrees while the loading angle was allowed to vary. A power ratio of 2.67×10^5 corresponds to a linear klystron. In Fig. 5b the threshold for beam loading with $\phi_z = -45$ degrees is plotted as a function of cavity voltage. For a linear klystron the threshold is constant near 2.

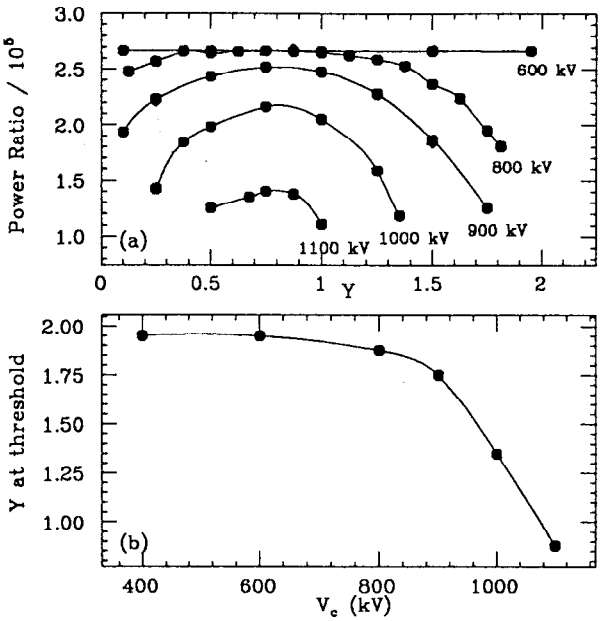

Figure 5. Ratio of the klystron output to input power as a function of loading ratio with $\phi_z = -45$ deg for different cavity voltages (fig. 5a) and stability threshold as a function of cavity voltage with $\phi_z = -45$ deg (fig. 5b). Higher order mode losses were assumed to be constant.

5. Conclusion

The equations of motion for the beam dynamics mixed to baseband were used to model the damping ring rf systems at the SLC. Measured feedback loop and klystron characteristics were included. Robustness of the simulations has been demonstrated by comparison to theory and experiment in the time and frequency domains. First results included a study of the nonlinear klystron. In the future we will study stability of the rf system with all the feedback loops closed.

The authors thank F. Pedersen of CERN, A. Hill, P. Correidoura, J. Judkins, and H. Schwartz of SLAC, and S. Karahan of Integrated Systems for their insights.

References

[1] P.Krejcik *et al*, "High Intensity Bunch Length Instabilities in the SLC Damping Rings", these proceedings

[2] F.Pedersen, "Beam Loading Effects in the CERN PS Booster", IEEE Tran. on Nucl. Sci., NS-22, No. 3 (1975) 1906.

[3] F.Pedersen, "A Novel RF Cavity Tuning Feedback Scheme for Heavy Beam Loading", IEEE Tran. on Nucl. Sci., NS-32, No. 3 (1985) 2138.

[4] P.Krejcik *et al*, 'RF Feedback for Beam Loading Compensation in the SLC Damping Rings", these proceedings

[5] Matrix-x by Integrated Systems, Santa Clara, CA

[6] Simulink by Mathworks, Boston, MA